IJCTA, 10(03), 2017, pp. 277-282

Travelling Wave Rotary Ultrasonic Motor with Novel Hollow Segments Stator

M.F.M. Sunif* and F.R.M. Romlay*

Abstract : This paper presents the method of determining and characterizing of a piezoelectric stator profile that applying in an ultrasonic motor with the consideration of heat that was generated. The ultrasonic motor is driven by the vibration of the piezoelectric element in order to ignite a motion. The harmonic and transient analysis methods are used to predict the optimized operation frequency of the ultrasonic motor travelling wave. Then, the thermal analysis was conducted in order to analyse the heat distribution on the stator. The ultrasonic motor showed a different longitudinal deflection with the increment of the temperature. Verification experiment is conducted through torque performance measurement. Travelling wave optimization was found to be strongly dependent on the heat that generated by piezoceramic material.

Keywords: Travelling wave; ultrasonic motor; stator.

1. INTRODUCTION

Motor is a device that is driven by electromagnetic force which involves conversion of electrical energy to mechanical energy [1]. On the other hand, ultrasonic motor is a device that is driven by piezoelectric vibrations to convert electrical energy to mechanical energy [2]. Ultrasonic motor consists of piezoceramic, electrode, stator and rotor as its components. The stator surface is coupled with piezoceramic and AC voltages are supplied through electrodes. The voltages displace the stator in an elliptical trajectory. In response to the stator displacement, the rotor rotates simultaneously [3, 16]. The travelling-wave piezoelectric ultrasonic motor (TWUSM) has recently been attracting considerable attention due to the high torque compare to the volume ratio, bigger torque at lower speed, long life span and high stability in use. Furthermore, ultrasonic motor provides free electromagnetic interference [4].

However, a lot of efforts were required to produce a robust ultrasonic motor. In the earlier development of ultrasonic motor, heat generation was not considered [5], [6], [7]. An overheating was caused depoling of the piezoceramic [8]. As a result, the motor is not suitable for continuous and long operation.

To overcome the heat problem, factors that caused heat generations were studied and reported [9]. Mathematical modelling of the temperature distribution was established using three-dimensional finite element method [10]. Devos *et al.* proved that the resonant mode working principal had reduced the heat dissipation [11]. However, a lot of heat is still generated and effective method to reduce the heat is still needed.

In order to reduce the generated heat of ultrasonic motor, heat distribution model for ultrasonic motor must be established. In this study, heat effect modelling of ultrasonic motor stator was developed. The top surface of the stator profile was modeled and analysed.

2. HEAT GENERATED BY ULTRASONIC MOTOR

The heat suppression of the piezoceramics is depending on the mechanical quality factor, Q which defined as a ratio of energy stored and loss for each of an oscillation [12]. With a high mechanical quality factor, Q, less heat was generated and this parameter must be taken into consideration [8].

* Faculty of Mechanical Engineering, Universiti Malaysia Pahang, 26600 Pekan, Pahang, Malaysia. *Email: fadhlur@ump.edu.my*

The generated heat during the vibrations influences dielectric loss of piezoceramic material. The relation of the piezoceramic temperature, T with the dielectric loss is shown as equation (1) [13].

$$T = T_o + \frac{R}{U} \tag{1}$$

where T_o is the ambient temperature, R is the thermal resistance of the dielectric and U is the voltage supplied. The thermal resistant, R is numerically appropriate to the temperature increment during the conversion into thermal energy.

The increment of the piezoceramics temperature was able to influence driving frequency, ω of the stator and the relation of both factors is given as [14]:

$$\omega = \omega_o(1-1.03\times10^{-4}(T-T_o)+0.77\times10^{-7}(T-T_o)^2)^{1/2} \tag{2}$$

where ω_o is a natural frequency. The heat that affects the frequency can influence displacement of the stator, u_z in a function of radius, *r*, angle, θ and time, *t* based on equation below [15].

$$u_z(r,\theta,t) = f(q)R(r)\cos(k\theta)e^{j(wt-\phi_k)} \tag{3}$$

where

$$R(r) = \left\{J_k\left(\alpha_k\frac{r}{a}\right)+C_kI_k\left(\alpha_k\frac{r}{a}\right)\right\}$$

$$f(q) = \frac{F_K}{\omega_k^2\sqrt{\left[1-(\omega/\omega_k)^2\right]^2+4\xi_k^2(\omega/\omega_k)^2}}$$

$$F_k = \frac{1}{\rho h N_k}\int_b^a\int_0^{2\pi}Q_3(r,\theta)R(r)\cos(k\theta)rdrd\theta$$

$$N_k = \int_b^a\int_0^{2\pi}[R(r)\cos(k\theta)]^2rdrd\theta$$

$$C_k = \frac{\alpha_k^2J_k(\alpha_k)+(1-\sigma)\left\{\alpha_kJ_k(\alpha_k)-k^2J_k(\alpha_k)\right\}}{\alpha_k^2I_k(\alpha_k)+(1-\sigma)\left\{\alpha_kI_k(\alpha_k)-k^2I_k(\alpha_k)\right\}}$$

The equations above integrate the properties such ξ_k denotes a modal damping coefficient, ϕ_k denotes a phase lag, α_k denotes a frequency constant and σ denotes a Poisson's ratio. On the other hand, geometry properties were represented by *b* which denotes an inner radius, a denotes an outer radius, *h* denotes a half-thickness of the plate, ρ denotes a mass density of the material, J_k denotes a Bessei functions and I_k denotes a modified Bessei functions.

3. METHODOLOGY OF ULTRASONIC MODELLING

Two structures of USR 6060 Shensei ultrasonic motor stator was used in the experiment of heat dissipation. The stators were made by copper material that divided into 90 pieces of segment and they are supported by piezeceramic at bottom side. One of the USR 6060 Shensei stator was modified by drilling holes at side surface for each divided segments as shown in Figure 1. The holes makes the stator segments appears as hollow geometry instead of solid. The design was considered as a novelty for ultrasonic motor stator.

Finite element analysis (FEA) was applied using MSC Marc Mentat software to simulate the vibration characteristic. Computational aided design (CAD) was developed by integrating 143 elements of piezoelectric material and 528 elements of 3-D solid. The elements were in hexagon shape.

The structure was simulated using harmonic mode analysis to identify the optimized frequency that provides the highest displacement on Z-axis. The range of the frequency is set from 1 to 50 kHz.

Figure 1: The structure of the stator of ultrasonic motor

Then, the optimum frequency of the harmonic analysis was used as an input for transient analysis. The transient analysis was further preceded by providing two sinusoidal input functions which were shifted 90° from each other. The transient analysis was run for 3 ms to see the vibration profile of the top stator surface.

4. RESULTS

Harmonic finite element analysis of USR 6060 Shensei ultrasonic motor stator was run and mode shape results were obtained. The optimized mode shape frequency was determined by analysing the highest Z-axis displacement. From this point of view, frequency 40.6 kHz was the optimized frequency that provides the highest Z-axis displacement.

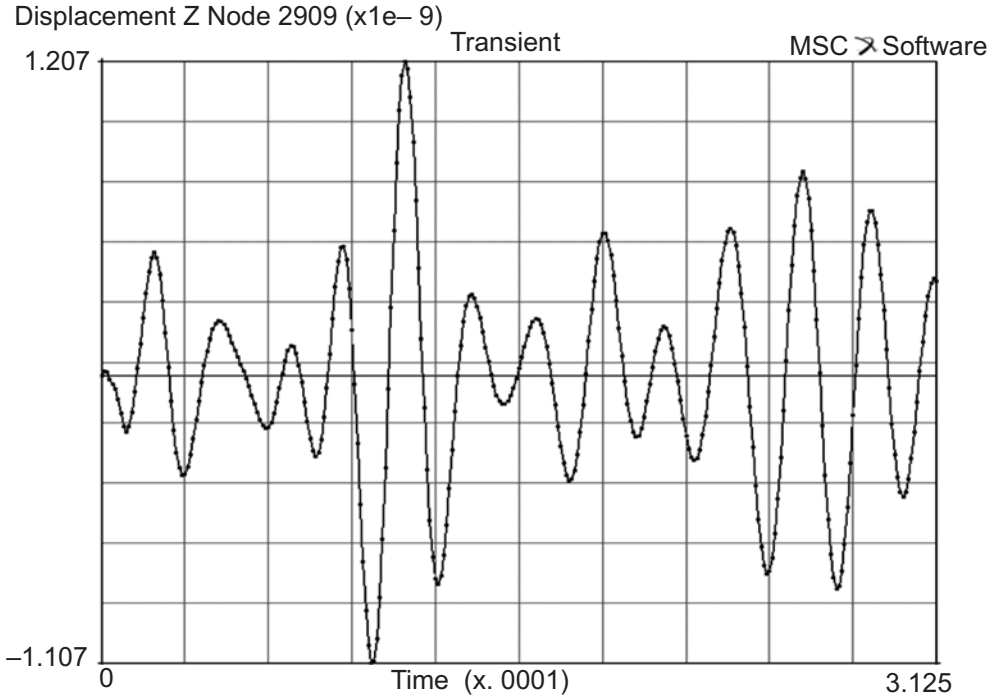

Figure 2: FEA of Z-axis displacement of node 2909 for Shensei stator

Based on harmonic analysis result, transient analysis at 40.6 Hz for USR6060 Shensei stator was run. The same frequency was applied for the hollow segments stator. The reason for using the same frequency was to investigate the effect of Z-axis displacements that cause by the hollow structure and not by other factor. For this purpose, Z-axis displacements for certain of period were established. The displacement profile for standard USR6060 Shensei stator and hollow segments stator were shown in Figure 2 and 3 respectively.

Stator profile that drives the rotor is interested and a local point at the top surface is selected. Node 2909 was chosen for further analysis.

Figure 2 shows the profile of the node 2909 for the USR6060 stator at 300 K temperature. This condition, which was closed at room temperature was considered as the initial stage of the ultrasonic motor operation. The maximum displacement that performed by the node 2909 at this condition is 1.207 nm.

The same condition was applied to the hollow segments stator. For the hollow segments stator, the maximum Z-axis displacement for node 2909 is 2.258 nm as given by Figure 3.

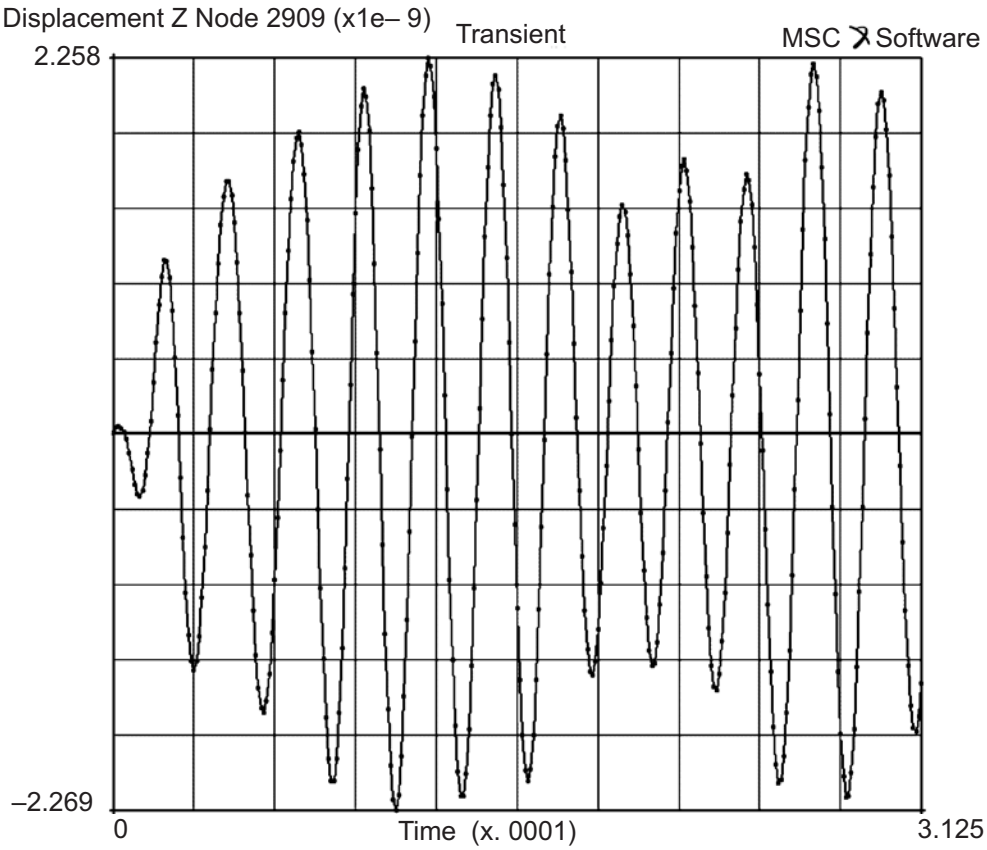

Figure 3: FEA of Z-axis displacement of node 2909 for hollow stator

It was shown that the hollow structure can influence the profile displacement of the ultrasonic motor stator. Indirectly, an addition of hollow shapes enables to improve the ultrasonic motor performance.

Since displacements have a relation with dissipated heat, heat transfer simulation and result verification were run through the temperature measurement experiment during the operation. The heat dissipation of USR 6060 Shensei and hollow segments stator were compared.

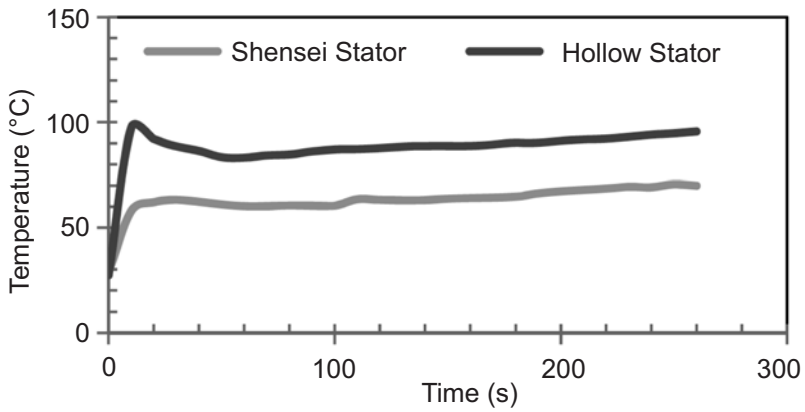

Figure 4: Stator temperature measured.

Through the experiment, hollow segments stator releases more heat compare to USR 6060 Shensei stator as illustrated in Figure 4. This happened because hollow segment stators have more surface area that allows more heat to dissipate. High dissipated heat means low heat was stored. The advantage reduces dielectric loss phenomena. The effect of the low loss, the save energy contributes to displacement profile amplitude. This would allow torque of ultrasonic motor to be improved.

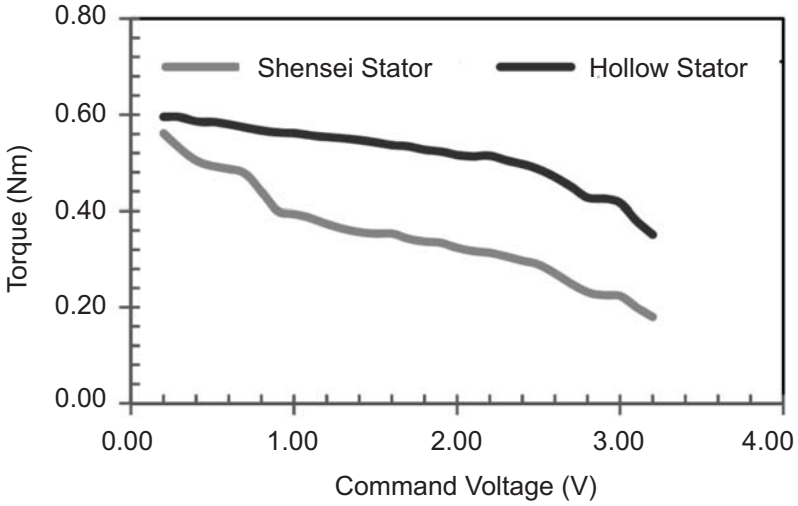

Figure 5: Torque performance of the ultrasonic motor

Figure 5 shows the hollow stator provides higher torque compare to the Shensei stator. The maximum torque of modified hollow stator was 0.60 Nm while Shensei stator was 0.58 Nm. The maximum torque was plotted at 0.20 V. The minimum torque for modified hollow stator was 0.36 Nm while Shensei stator was 0.20 Nm. The minimum torque was plotted at 3.20 V of the input signal. The torque experiment verified the finding accordingly.

5. CONCLUSION

As the conclusion, the dielectric loss that converted into heat can significantly influence the Z-axis displacement. A better way of controlling the dielectric loss will determine the stator surface deflection and directly contributed to the ultrasonic motor torque and speed improvement.

In order to gain the highest Z-axis displacement, the heat flux of the stator needs to be increased. By increasing the rate of the heat release, ultrasonic motor can provide a better performance.

It is suggested that the model of ultrasonic motor stator need to be verified through speed characteristic. Therefore, the rotor performance needs to put into account. This characteristic will determine the ultrasonic motor performance in overall.

6. ACKNOWLEDGEMENT

This work has been supported by the E-Science fund, Ministry of Science and Technology Malaysia. Support from the Nanotechnology Centre, Cranfield University, U.K. through research visiting program is also acknowledged.

7. REFERENCES

1. Cho C. P. and William P. K., (1996). Feasibility Study of a Novel Integrated Electric Motor/Pump for Underwater Applications, *Naval Engineers Journal,* **108**(3), pp. 233–242.

2. Nakamura, K., Kurosawa, M., and Ueha, S., (1993). Design of a Hybrid Transducer Type Ultrasonic Motor, *IEEE Transactions on Ultrasonics, Ferroelectrics and Frequency Control,* **40(**4).

3. Bar-Cohen, Y., Bao X. and Grandia, W., (1998). Rotary Ultrasonic Motors Actuated by Travelling Flexural Waves, *Proceedings of the Smart Structures and Materials Symposium, San Diego, CA,* **82**, pp. 3329-3335.

4. Sun, D., Liu, J. and Ai, X., (2002). Modeling and Performance Evaluation of Travelling-Wave Piezoelectric Ultrasonic Motors with Analytical Method, *Sensors Actuators A Physical*, **100**, pp. 84-93.
5. Wang, X., Shen, Y., **(**2001). A Solution of the Elliptical Piezoelectric Inclusion Problem under Uniform Heat Flux, *Int. Journal of Solids and Structures*, **38**, pp. 2503-2516.
6. Carlos, C. C. G., (2007). *Modeling and Experimental Validation of an Ultrasonic Rotary Motor,* Concordia University, Montreal, Quebec Canada.
7. Giraud F., (2010), Practical Considerations in Ultrasonic Motor Selection, *14th International Power Electronics and Motion Control Conference*, pp. 41-44.
8. Uchino, K., (1998). Piezoelectric Ultrasonic Motor: Overview, *Smart Material Structures*, **7**, pp. 273–285.
9. Chen, W. P., Chong, C. P., Chan, H. L.W. and Liu, P. C. K., (2003). Degradation in Lead Zirconate Titanate Piezoelectric Ceramics by High Power Resonant Driving, *Materials Science and Engineering B*, **99,** pp. 203–206.
10. Shiyang, L., and Ming, Y., (2010). Analysis of the temperature field distribution for piezoelectric plate-type ultrasonic ultrasonic motor, *Sensors and Actuators A: Physical*, **164**, pp. 107–115.
11. Devos, S., Reynaerts, D. And Brussel, H. V., (2008). Minimising Heat Dissipation in Ultrasonic Piezomotors by Working in a Resonant Mode, *Precision Engineering*, **32**(2), pp. 114-125.
12. Nawrodt, R., Zimmer, A., Nietzsche, S., Thürk, M., Vodel, W. and Seidel, P., (2006), A New Apparatus for Mechanical Q-Factor Measurements between 5 and 300 K, *Cryogenics*, **46**(10), pp. 718-723.
13. Bogomol'nyi, V. M., (1998), Calculation of Energy Dissipation and Temperature Rise of Piezoelectric Metal-Insulator-Metal Structures, *Measurement Techniques*, **41**(12). pp. 1162-1166.
14. Xu, X., Liang, Y. C., Lee, H. P., Lin W. Z., Lim, S.P., Lee, K.H. and Shi, X. H., (2003). Mechanical Modeling of Longitudinal Oscillation Ultrasonic Motors and Temperature Effect Analysis, *Smart Materials and Structures*, **12**, pp. 514-523.
15. Ming, Y. and Peiwen, Q. (2001). Performances Estimation of a Rotary Travelling Wave Ultrasonic Motor based on Two-Dimensional Analytical.
16. N. Semsri., C. Torasa., K. Samerjai., M. Suksombat and P. Sinpeng, "Electricity-generating wind turbine from electric bicycle motor," International Journal of Technology and Engineering Studies, vol. 2, no. 4, pp. 101-109, 2016. Model, *Ultrasonics*, **39,** pp. 115-120.